Fast Identification of Novel Lymphoid Tyrosine Phosphatase Inhibitors Using Target-Ligand Interaction-Based Virtual Screening

Supplementary Material

Xuben Hou,[†,#] Rong Li,[‡,#] Kangshuai Li,[§] Xiao Yu,[§] Jin-peng Sun,[‡,] and Hao Fang[†,*]*

Contents:

1. Chemical structures of inactive compounds.

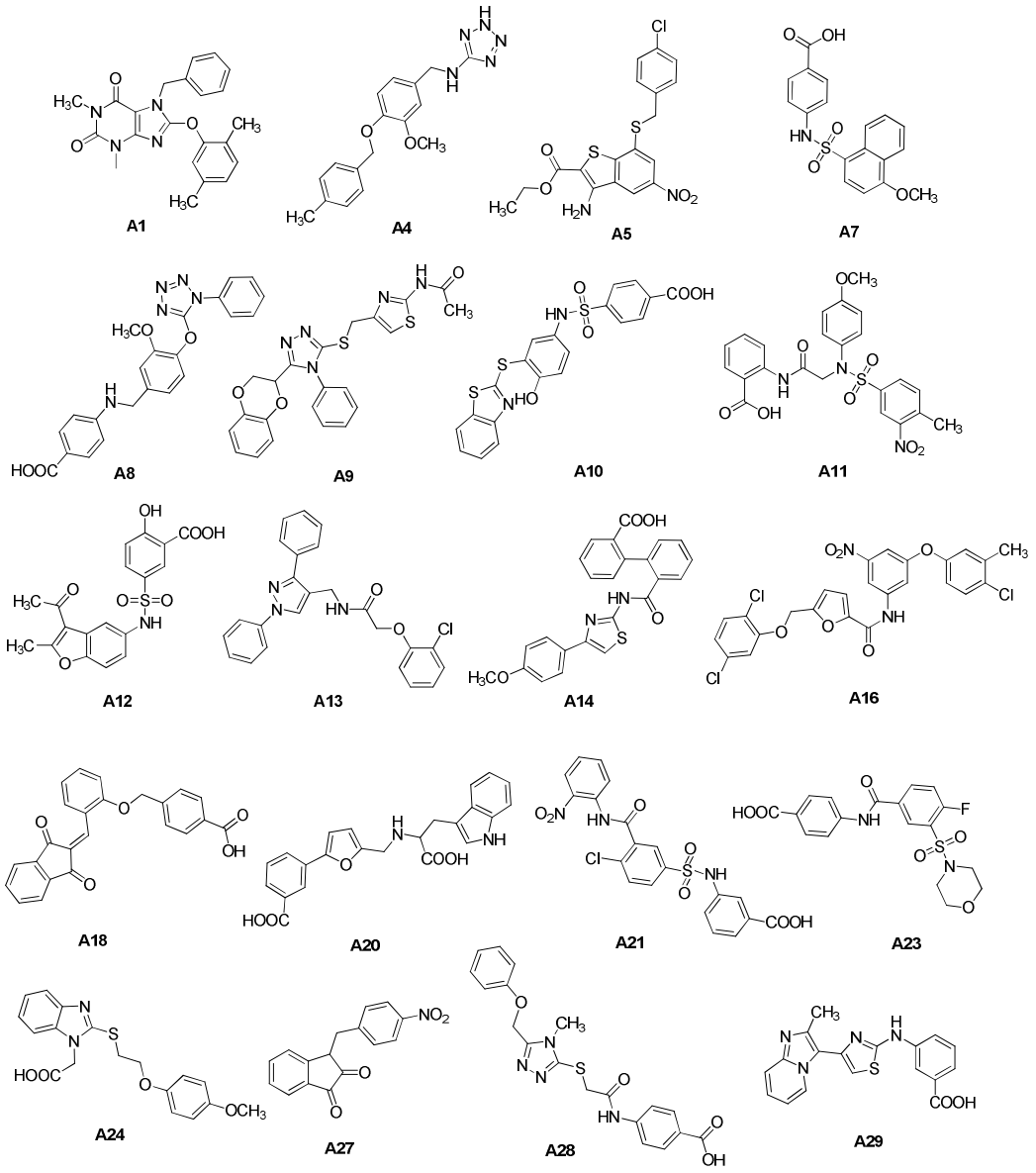

Figure S1. Chemical structures of selected compounds with IC_{50} higher than 100 μ M

2. Lyp inhibition, ranks, MS data and purity for selected 29 compounds.

Table S1. Docking-based rankings, MS data and purity data.

Name	Specs ID[a]	GoldScore Fitness	IC_{50}(μM)	Rank	ES-MS Positive (m/z) [a]	t_R (min) [a]	HPLC purity (%)[a]
A1	AO-343/41781084	56.67	>60	195	391.2	4.39	>95.0
A2	AE-641/37091012	61.75	**11.4±0.7**	109	499.3	3.57	>95.0
A3	AO-299/41409126	59.41	**31.6±6.8**	111	434.3	3.97	96.74
A4	AN-465/42888694	51.95	>60	214	326.24	3.25	>95.0
A5	AK-968/41922688	68.64	>60	59	423.1	5.21	97.61
A6	AN-023/13177206	72.89	**30.5±9.1**	52	462.2	4.01	>95.0
A7	AP-263/43371386	62.57	>60	92	357.07	3.2	>95.0
A8	AN-465/43384104	75.47	>60	29	418.3	3.72	>95.0
A9	AO-080/43441851	59.70	>60	63	465.93	0.84	>95.0
A10	AQ-390/42869319	64.24	>60	41	459.2	3.23	>95.0
A11	AG-690/15429642	64.40	>60	45	500.4	3.99	96.94
A12	AQ-390/43238281	53.64	>60	201	390.3	3.48	>95.0
A13	AK-968/40940879	58.78	>60	147	418.5	4.44	>95.0
A14	AG-690/09684006	67.64	>60	55	431.1	4.03	>95.0
A15	AO-081/15385001	58.88	**6.1±1.1**	84	598.3	4.81	>95.0
A16	AK-968/41925005	69.58	>60	45	-	^{1}H-NMR data[b]	
A17	AK-968/15256501	80.26	**36.6±7.7**	31	-	^{1}H-NMR data[b]	
A18	AM-879/40965082	77.32	>60	18	358.0	4.15	96.41
A19	AQ-088/42014071	52.97	**18.5±3.1**	152	589.9	4.53	96.16
A20	AN-465/43411028	66.81	>60	89	405.13	0.57	97.04
A21	AH-034/11365849	71.99	>60	15	476.0	3.56	>95.0
A22	AN-465/14952274	68.50	**37.1±7.2**	71	441.0	4.96	99.34
A23	AG-205/12140185	62.54	>60	124	409.2	3.27	>95.0
A24	AG-690/36897006	53.37	>60	248	-	^{1}H-NMR data[b]	
A25	AF-399/42048252	68.01	**55.9±4.4**	57	436.4	3.76	>95.0
A26	AN-648/42098518	54.93	**20.5±3.3**	77	493.1	4.00	96.74
A27	AG-690/09407063	55.50	>60	159	-	^{1}H-NMR data[b]	
A28	AN-698/42147479	52.44	>60	217	399.2	3.08	>95.0
A29	AG-205/13579050	55.01	>60	135	351.1	0.40	>95.0

[a] The chemical structures MS data and HPLC data are available on the Specs website (www.specs.net).

[b] Purities were confirmed using ^{1}H-NMR, data available on the Specs website (www.specs.net).

3. MS data and HPLC purity for derivatives of A15 and A19.

Table S2. Lyp inhibition, MS data and purity data for derivatives of A15 and A19.

Name	Specs ID[a]	IC_{50}(μM)	ES-MS Positive (m/z) [a]	t_R (min) [a]	HPLC purity (%)[a]
A15-1	AN-648/15596073	**42.0±13.7**	479.3	4.96	97.9
A15-2	AN-648/14910004	**36.5±12.0**	479.3	4.01	>99
A15-3	AN-648/15596181	**79.5±13.0**	556.0	3.81	>99
A15-4	AH-487/11778085	>100	-	^{1}H-NMR data[b]	
A15-5	AN-648/15596202	**7.1±2.6**	615.3	4.47	97.6
A19-1	AQ-088/41967335	**39.2±4.9**	568.1	4.28	>99
A19-2	AQ-088/41967395	**41.7±3.4**	644.1	5.01	97.0
A19-3	AQ-088/42014085	**41.36±12.7**	598.1	4.73	>99
A19-4	AQ-088/42014093	**27.6±7.6**	578.2	4.76	90.8
A19-5	AQ-088/42014116	>100	460.1	4.12	95.4
A19-6	AG-205/36485033	**48.7±10.4**	536.0	4.62	>99
A19-7	AQ-088/41085728	>100	398.3	3.24	>99
A19-8	AG-205/12230087	>100	504.0	4.42	97.9
A19-9	AG-205/36915235	>100	639.3	3.83	>99

[a] The chemical structures MS data and HPLC data are available on the Specs website (www.specs.net).

[b] Purities were confirmed using ^{1}H-NMR, data available on the Specs website (www.specs.net).

4. The Lineweaver-Burk plots of A3, A6, A17 and A22.

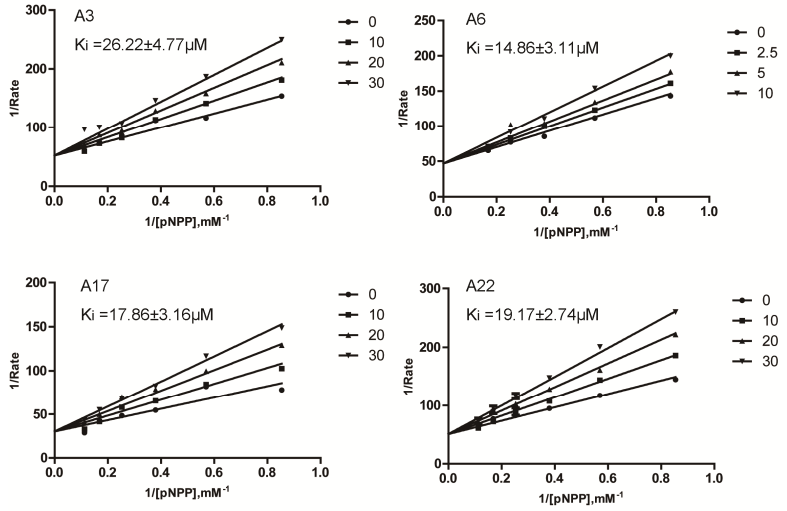

Figure S2. Kinetic analysis of Lyp inhibition by A3, A6, A17 and A22. The Lineweaver-Burk plot displayed the characteristic pattern of intersecting lines, which indicates competitive inhibition. The experiments were conducted at 25 °C, pH 7.0, with an ionic strength of 0.15 M, adjusted by NaCl.

5. Structure similarity analyze of nine novel inhibitors

To evaluate the novelty of these nine inhibitors with respect to known Lyp inhibitors (**8b**[1], **I-C11**[2], **LTV-1**[3] and **4e**[4]), the Tanimoto similarity indices (T)[5, 6] based on the FCFP_4 fingerprints were calculated using Fingerprints protocol in Discovery Studio 2.5. The Tanimoto coefficient is the well-known method of choice for the computation of fingerprint-based similarity in terms of a distance measure, giving values in the range of zero (no bits in common) to unity (all bits the same). Typically, structures with T > 0.85 are considered similar.[7] The results showed that these nine inhibitors all have low Tanimoto similarity values (less than 0.3) compared with the known inhibitors (Table S2).

Table S3. Similarity of nine novel inhibitors compared with four known Lyp inhibitors

	Tanimoto similarity (T)[a]			
	8b	**I-C11**	**LTV-1**	**4e**
A2	0.19	0.11	0.17	0.06
A3	0.16	0.11	0.19	0.13
A6	0.14	0.13	0.05	0.07
A15	0.11	0.07	0.27	0.06
A17	0.15	0.14	0.12	0.09
A19	0.13	0.09	0.18	0.12
A22	0.15	0.12	0.10	0.10
A25	0.14	0.09	0.15	0.08
A26	0.18	0.08	0.28	0.07

[a] Tanimoto similarity were calculated following equation S1:

$SA/(SA+SB+SC)$ (Eq S1)

(*SA*: The number of bits present in both the target and the reference; *SB*: The number of bits in the target but not the reference; *SC*: The number of bits in the reference but not the target.)

6. Redock studies using Lyp-8b co-crystal structure.

Table S4. RMSDs calculated between crystal structure and docked conformations.

Docking Program	Score Functions	RMSD
LigandFit	LigScore-1	9.21
	LigScore-2	9.21
	PLP1	9.15
	PLP2	9.21
	Jain	9.43
	PMF	9.10
	DockScore	9.46
Surflex	TotalScore	2.23
Gold	GoldScore	1.54
	ChemScore	4.57
Glide	G-Score(HTVs)	1.55
	G-Score(SP)	1.71

7. Calculated molecular properties of A2, A15, A19 and A26.

Table S5. LogP and PSA values of active compounds as well as reported inhibitors.

Compound	A2	A15	A19	**8b**	**LTV-1**
XLogP [a8]	4.65	1.89	1.85	2.78	3.04
ALogP [b]	7.251	5.811	5.869	3.802	5.229
PSA [c]	70.638	125.363	140.074	121.874	125.299

[a] Calculated with XLogP version 3.0;

[b] Calculated with Discovery Studio version 2.5;

[c]Calculated with QikProp;

8. IC_{50} curves for the four most active hits against a panel of protein phosphatases. (IC_{50} > 100μM were not shown)

Graph shows concentration-dependent inhibition of the four most active hits against a panel of protein phosphatases. Plot shows the protein phosphatases-catalyzed hydrolysis of the pNPP versus inhibitor concentration. Lines are fitting of the data to Eq. 2 for the purpose of calculating the IC_{50} values.

$$A_I = A_0 * IC_{50} / \left(IC_{50} + [I] \right) \qquad \text{Eq. 2}$$

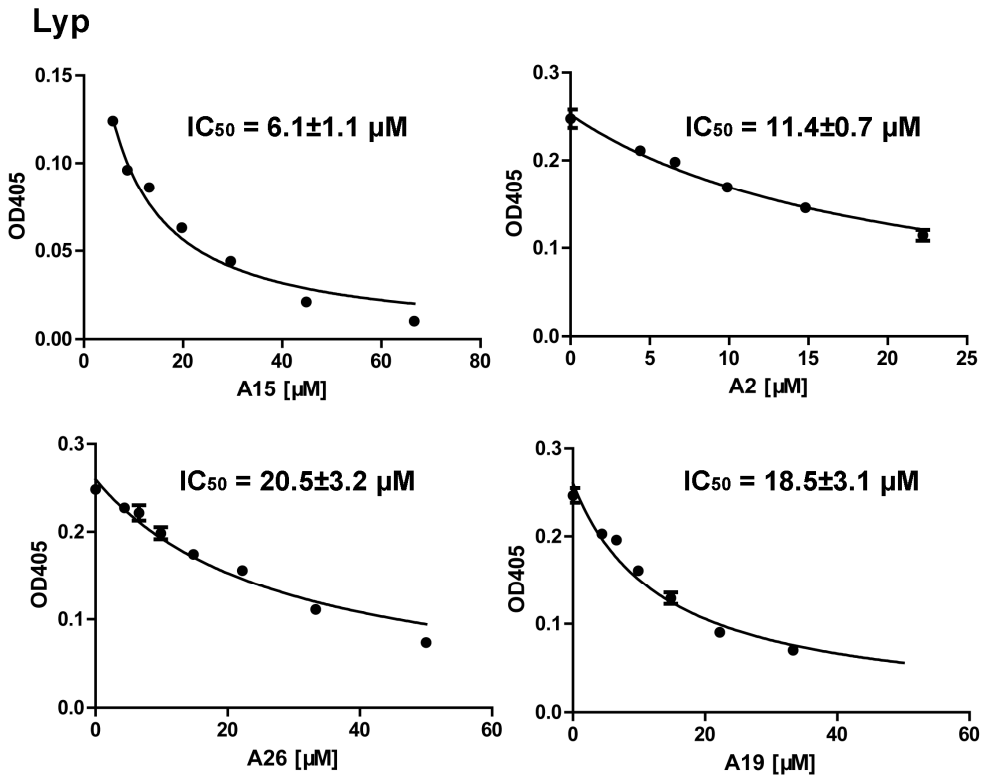

Figure S3. Inhibition curves used to determine the IC_{50} values for compound A15, A2, A26 and A19 against Lyp.

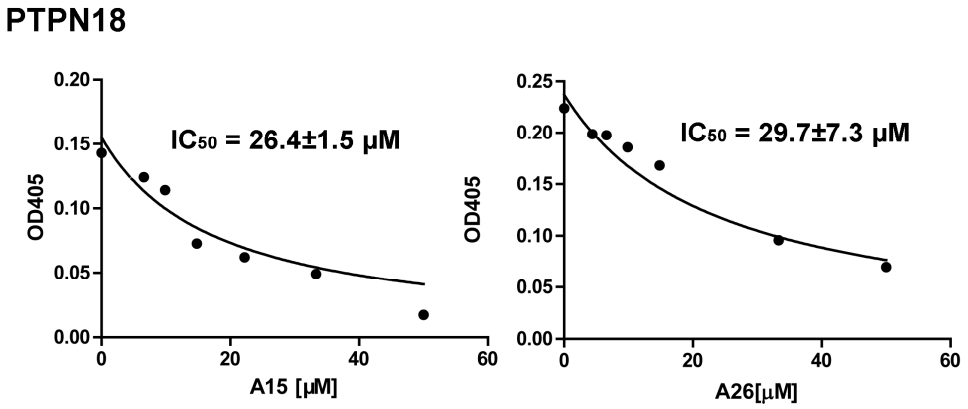

Figure S4. Inhibition curves used to determine the IC_{50} values for compound A15 and A26 against PTPN18.

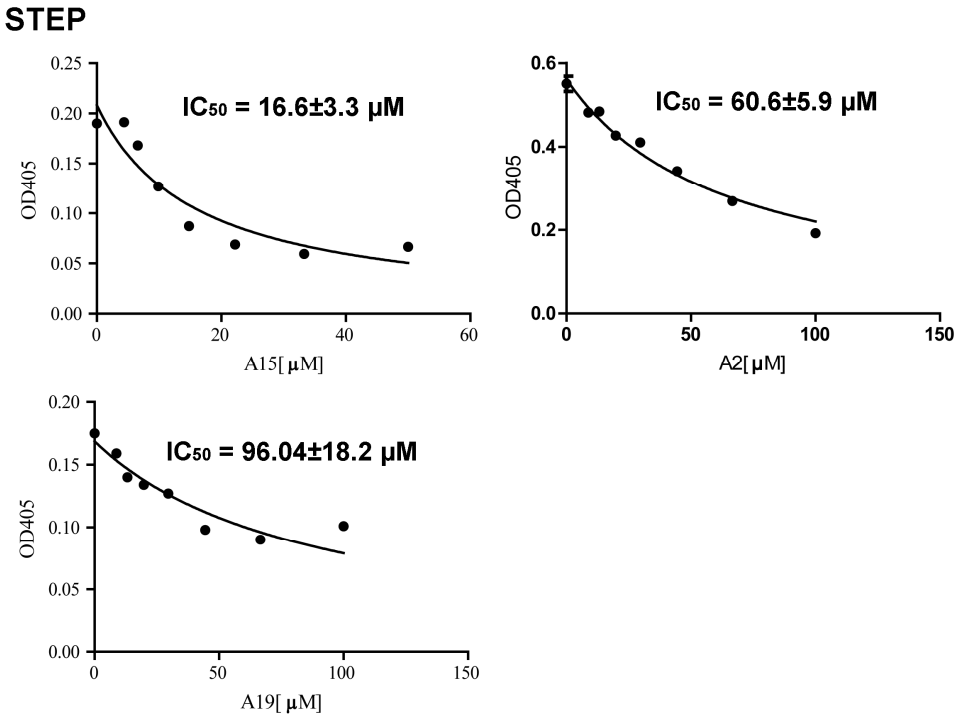

Figure S5. Inhibition curves used to determine the IC_{50} values for compound A15, A2 and A19 against STEP.

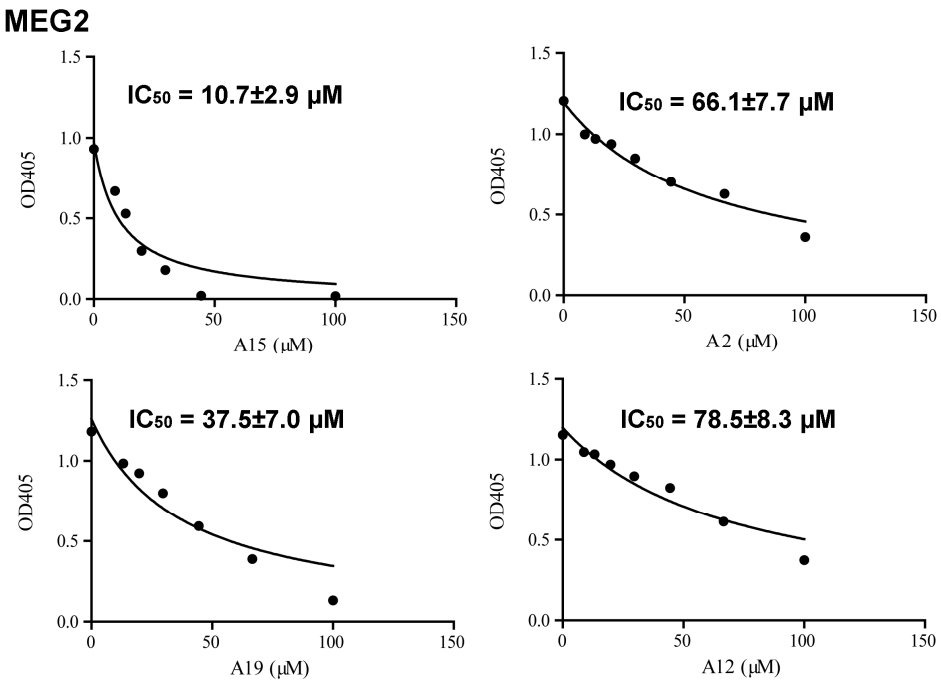

Figure S6. Inhibition curves used to determine the IC_{50} values for compound A15, A2, A26 and A19 against MEG2.

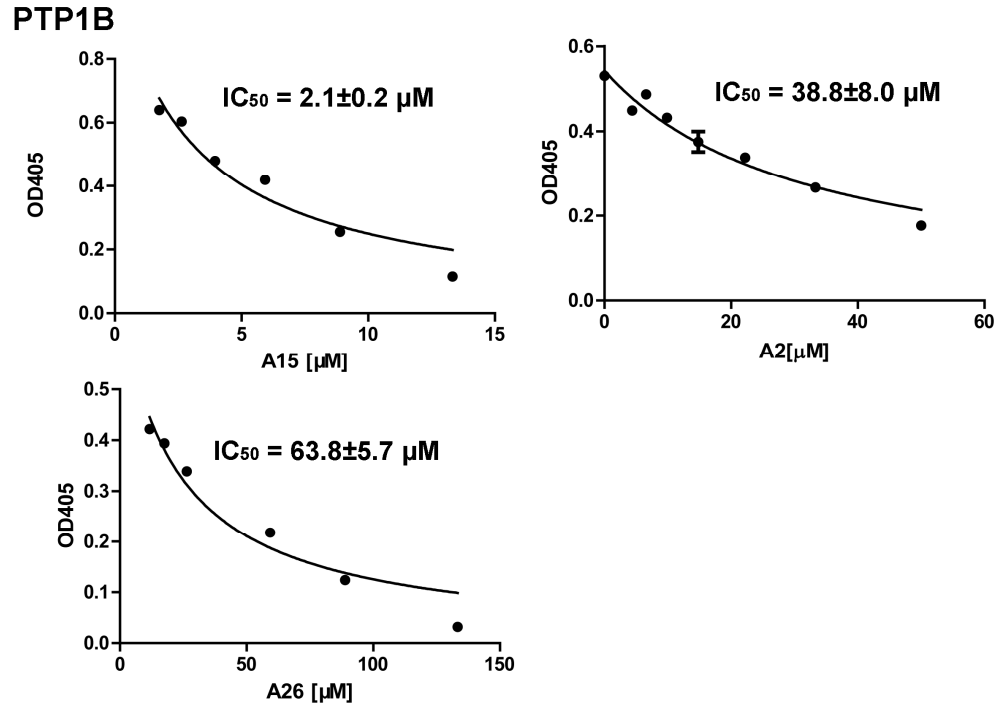

Figure S7. Inhibition curves used to determine the IC_{50} values for compound A15, A2 and A26 against PTP1B.

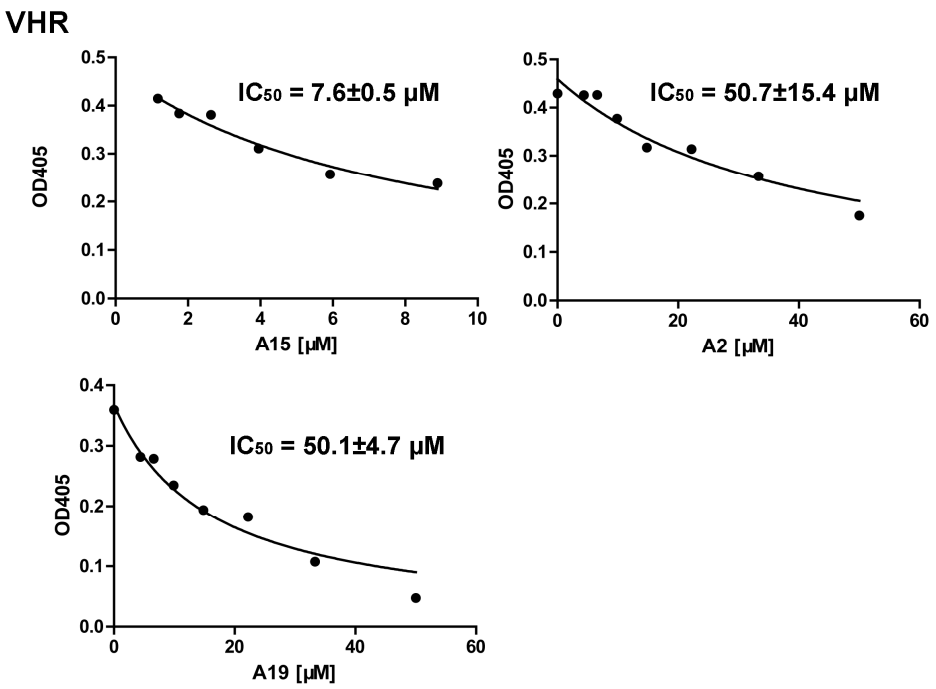

Figure S8. Inhibition curves used to determine the IC_{50} values for compound A15, A2 and A19 against VHR.

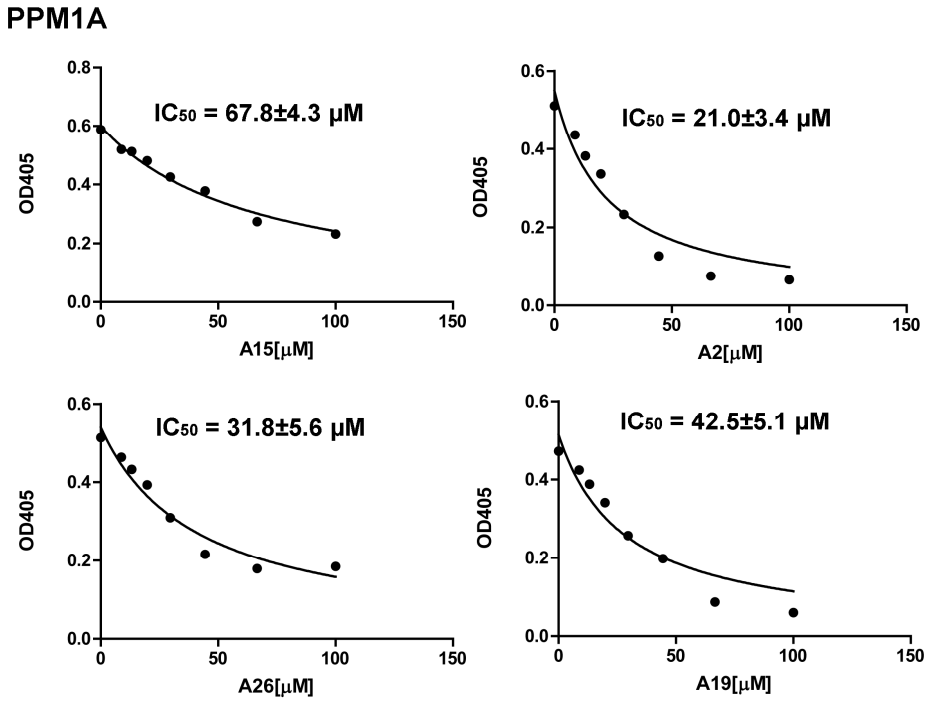

Figure S9. Inhibition curves used to determine the IC_{50} values for compound A15, A2, A26 and A19 against PPM1A.

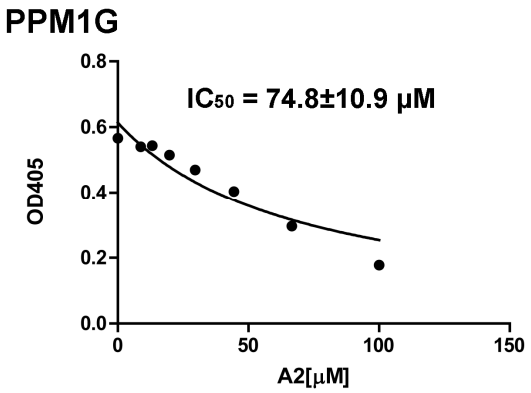

Figure S10. Inhibition curves used to determine the IC_{50} values for compound A2 against PPM1G.

6. Reversible binding of compound A2, **A3**, **A15**, **A19, A22, A25** and **A26.**

Reversible binding of seven compounds (**A2**, **A3**, **A15**, **A19, A22, A25** and **A26**) were examined by varying the pre-incubation time of Lyp inhibitors, in order to determine whether there is a time-dependent inhibition. Lyp were pre-incubated with these inhibitors at a concentration of 40μM, and the time-depended ratio of K_{cat} (control)/K_{cat} (inhibitor) were determined. Irreversibly binding could lead to the decrease of K_{cat} (inhibitor) as time, whereas the K_{cat} (inhibitor) remain constant when the inhibitor binding reversible[9]. As shown in Figure S11, most of these compounds bound Lyp reversibly with no increase in the ratio of K_{cat} (control) over K_{cat} (inhibitor) over 10–40 min of preincubation, except for compound **A25**, which showed covalent inhibition against Lyp.

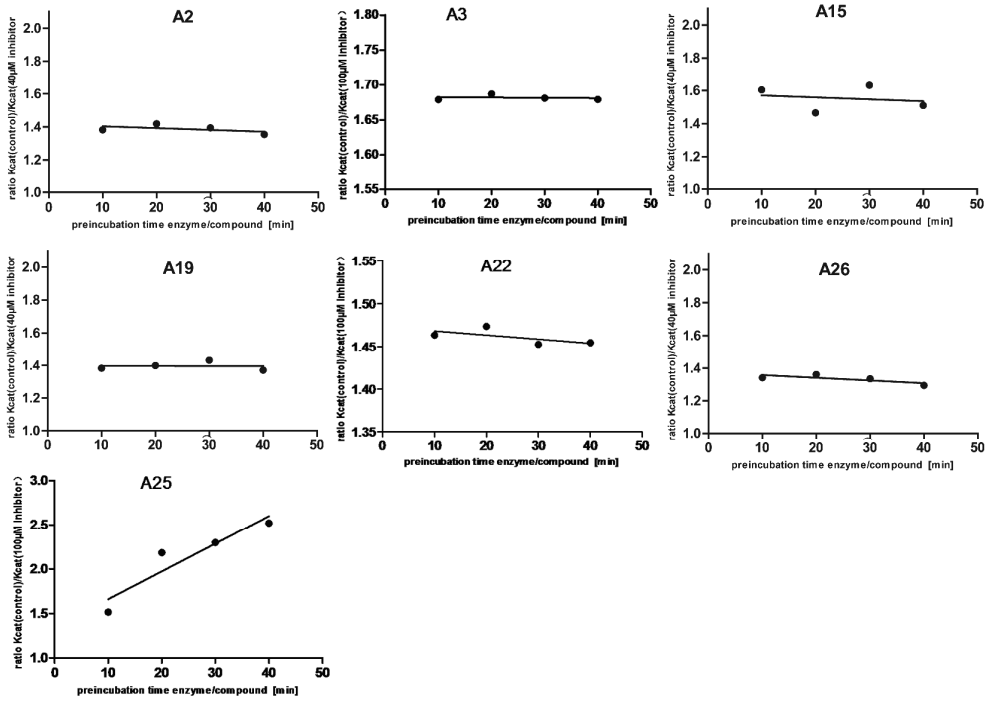

Figure S11. The time-depended ratios of Kcat (control)/Kcat (inhibitor).

10. Kinetic parameters for covalent Lyp inhibitor A25.

Consider the fact that the Lyp inhibition by compound **A25** is time-dependent, we carried out a detailed kinetic analysis of the interaction between compound **A25** and the catalytic domain of Lyp. By fitting the k_{obs} values as a function of inhibitor concentration, we observed saturation kinetics as shown in Figure 2, and calculated the kinetic constants K_i=40.98±13.19 μM and k_{inact}=0.1263±0.0117 min^{-1} for compound **A25**.

Method:

Lyp inactivation by **A25** was measured as described [10]. Inhibitor **A25** at various concentrations were added (30μL) to the wells of a 96-well plate containing 50 mM 3,3-dimethylglutarate buffer, and the ionic strength of 0.15 M was adjusted with NaCl. A 30 μL of Lyp in the same buffer was added to the wells. At appropriate time intervals，the reaction was initiated by addition of 4 Mm pNPP to a reaction mixture containing Lyp and **A25**, and stopped by addition of 1 M NaOH. The kinetic parameters of the inactivation reaction were obtained by fitting the data to the following equations:

$$\frac{A_t}{A_0} = \frac{A_\infty}{A_0} - \left(\frac{A_0 - A_\infty}{A_0}\right) e^{-K_{obs} \bullet t} \qquad K_{obs} = \frac{k_{inact} \bullet [I]}{K_i + [I]}$$

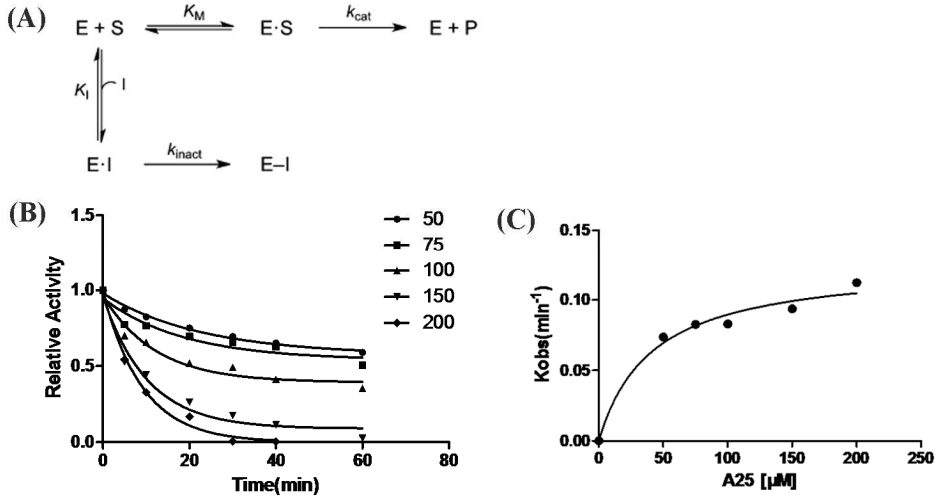

Figure S12. (A) Equation illustrating the irreversible inhibition of an enzyme. (B) Time-dependent inhibition of Lyp by compound A25. (C) The kobs data of A25 at different concentrations.

11. Proposed binding modes of A3, A6, A17, A22 and A25.

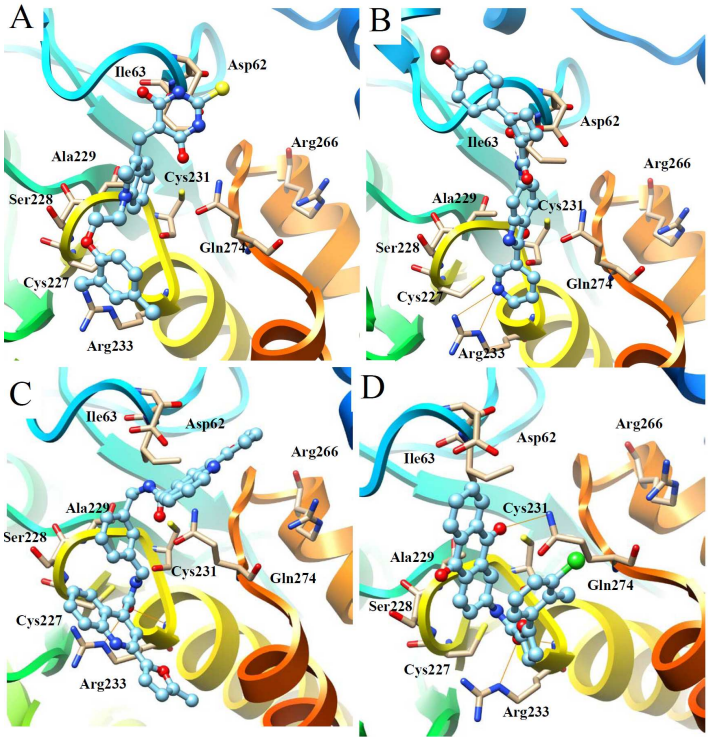

Figure S13. Proposed binding modes of A3 (A), A6 (B), A17 (C), A22 (D) and A25 (E).

12. Pharmacophore mapping of A15, A2, A19 and A26.

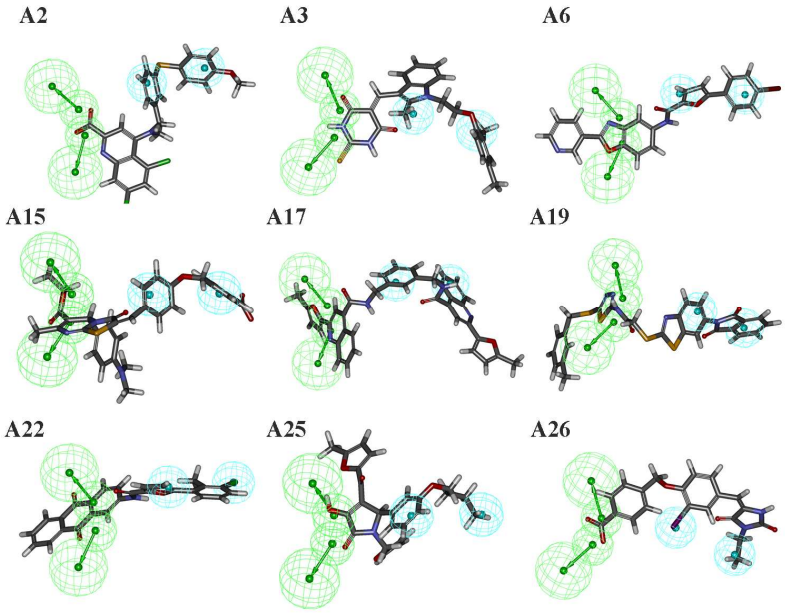

Figure S14. Pharmacophore mapping of nice active hits.

13. Protein phosphatases quality assurance.

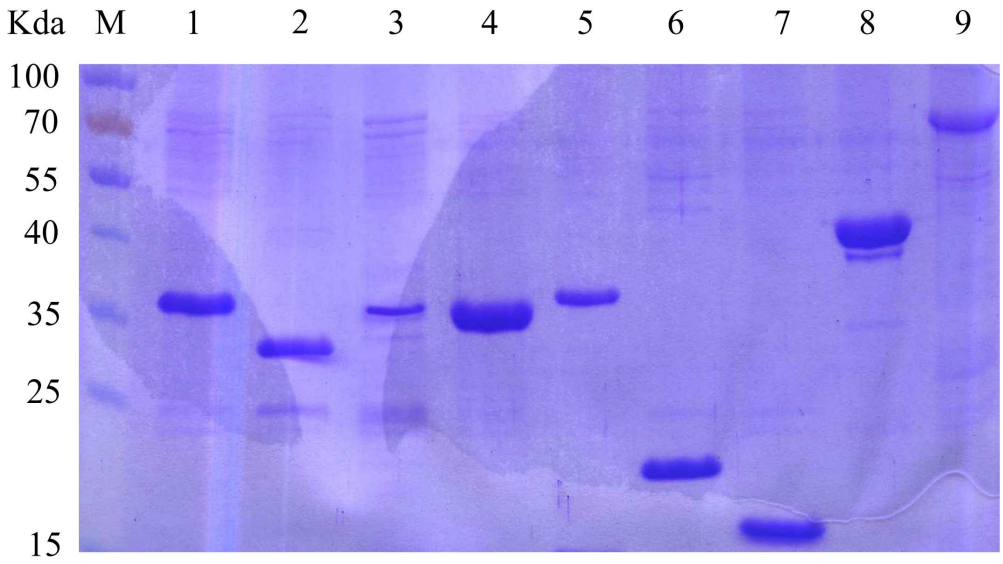

Figure S15. Protein phosphatases quality assurance.

M: SDS-PAGE Protein Marker;

Lane 1: Lyp protein;

Lane 2: PTPN18 protein;

Lane 3: STEP protein;

Lane 4: MEG2 protein;

Lane 5: PTP1B protein;

Lane 6: VHR protein;

Lane 7: SSH2 protein;

Lane 8: PPM1A protein;

Lane 9: PPM1G protein.

14. ^{1}H NMR spectra for selected compounds.

Compound A2

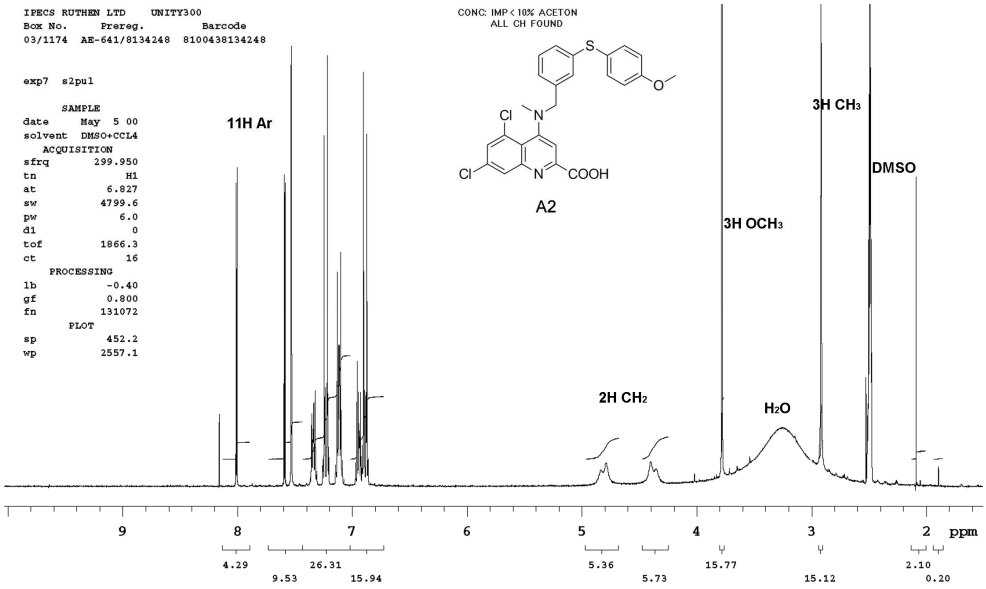

Compound A3

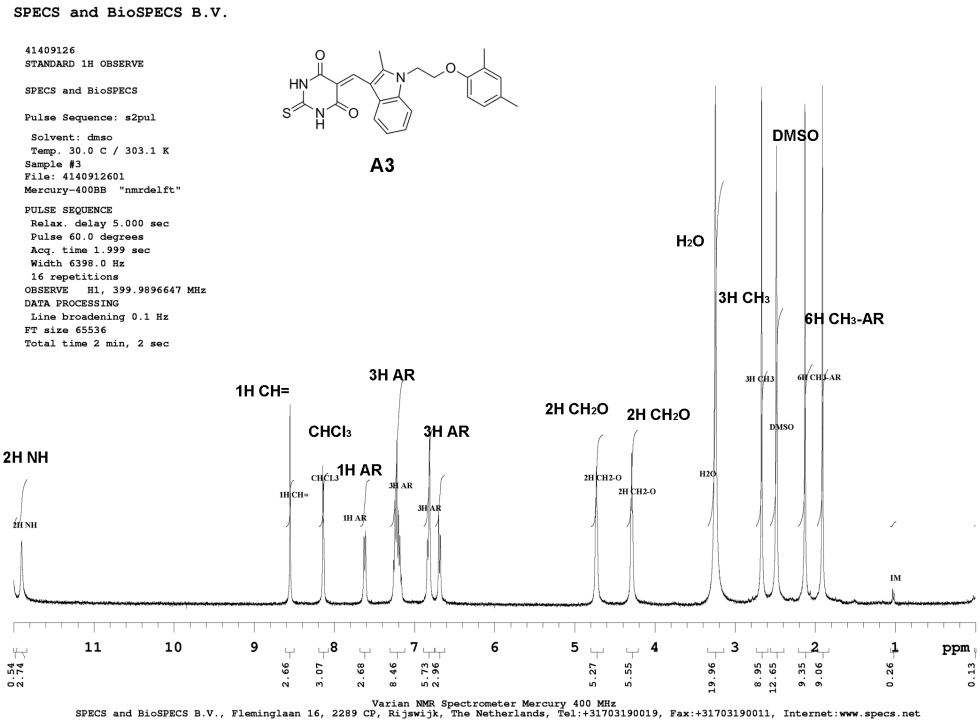

Compound A6

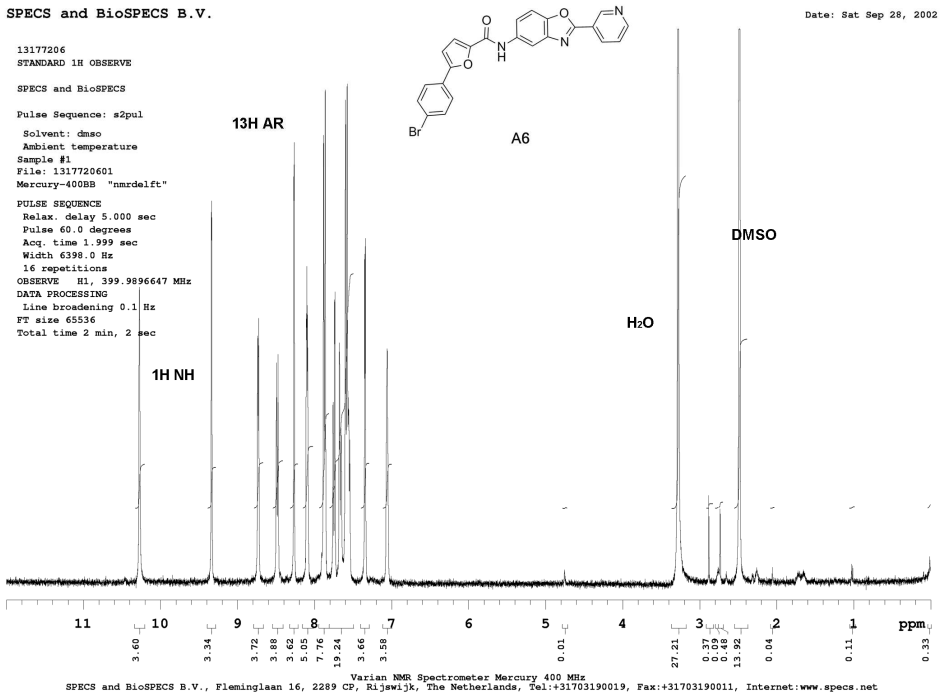

Compound A15

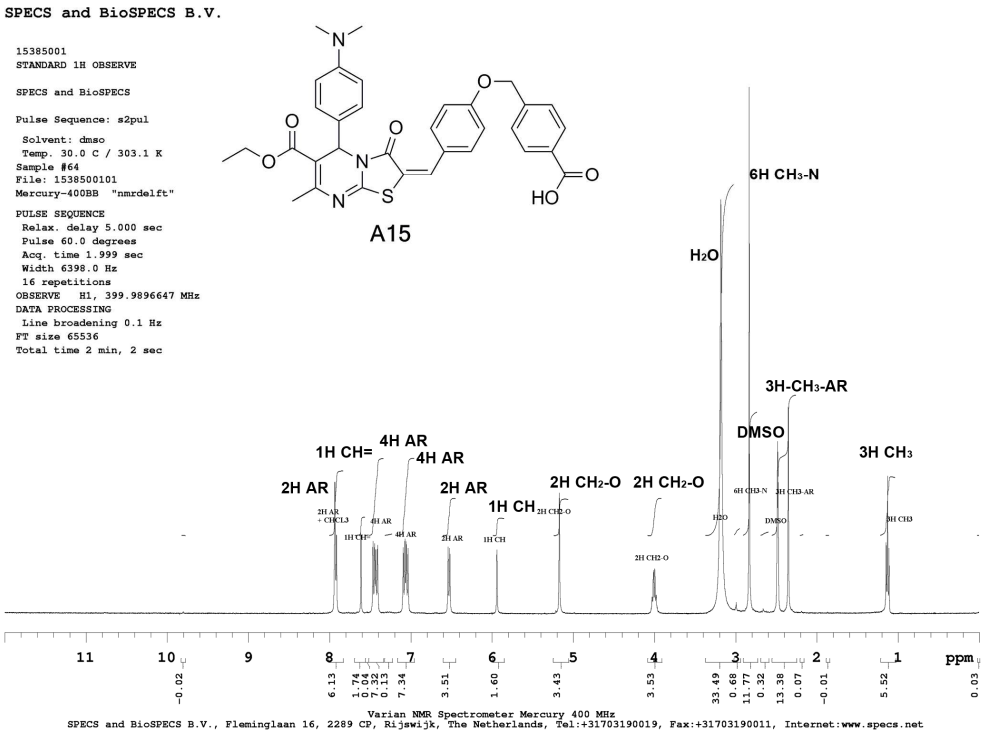

Compound A17

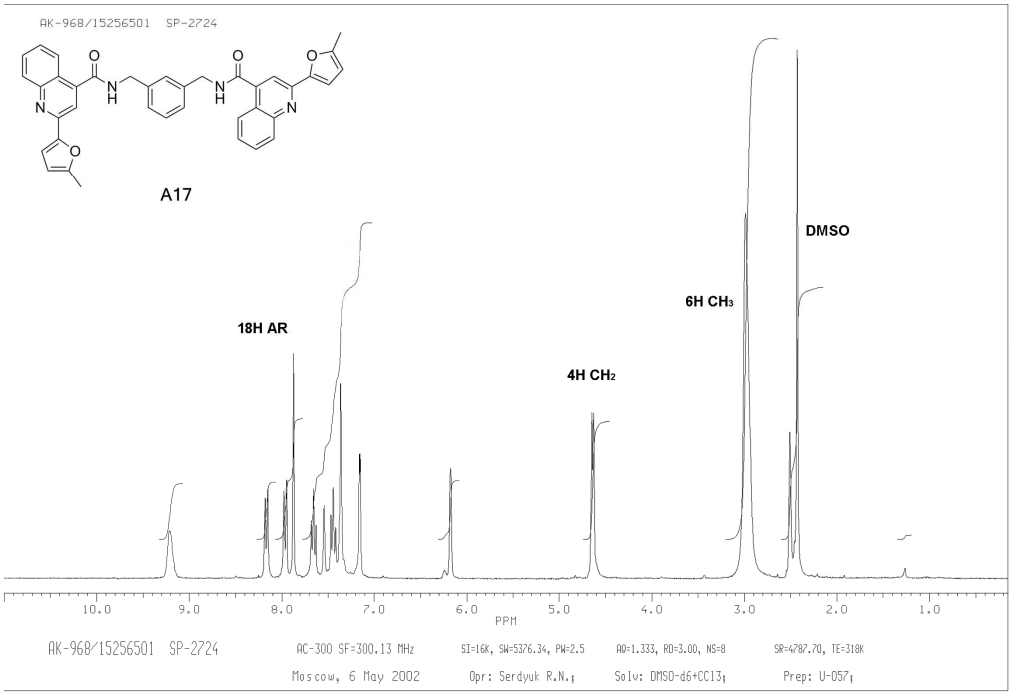

Compound A19

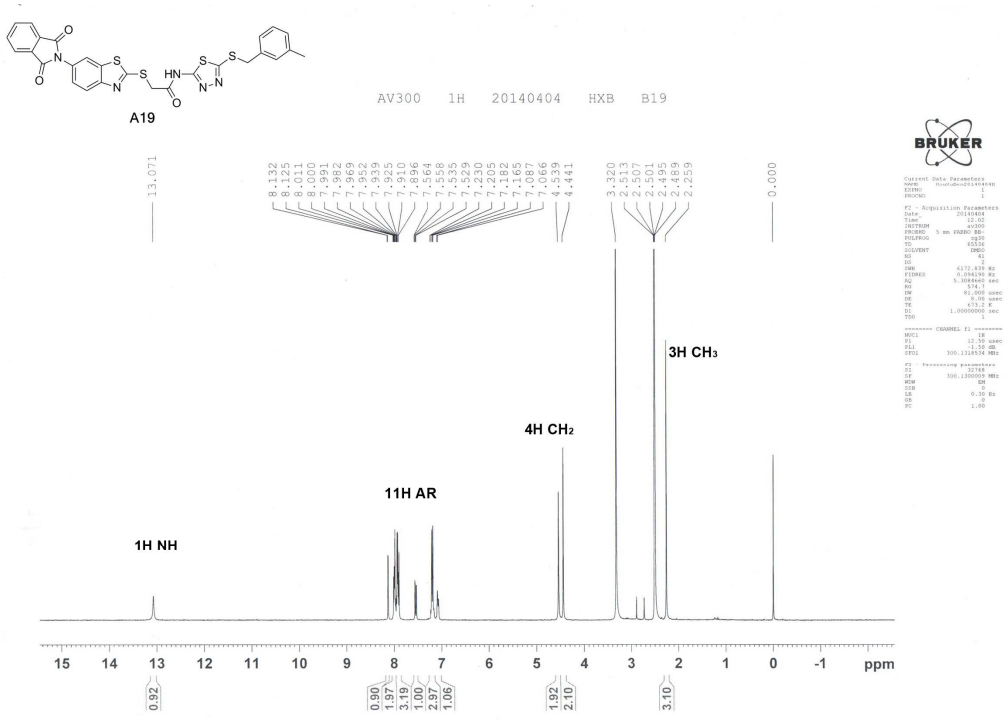

Compound A22

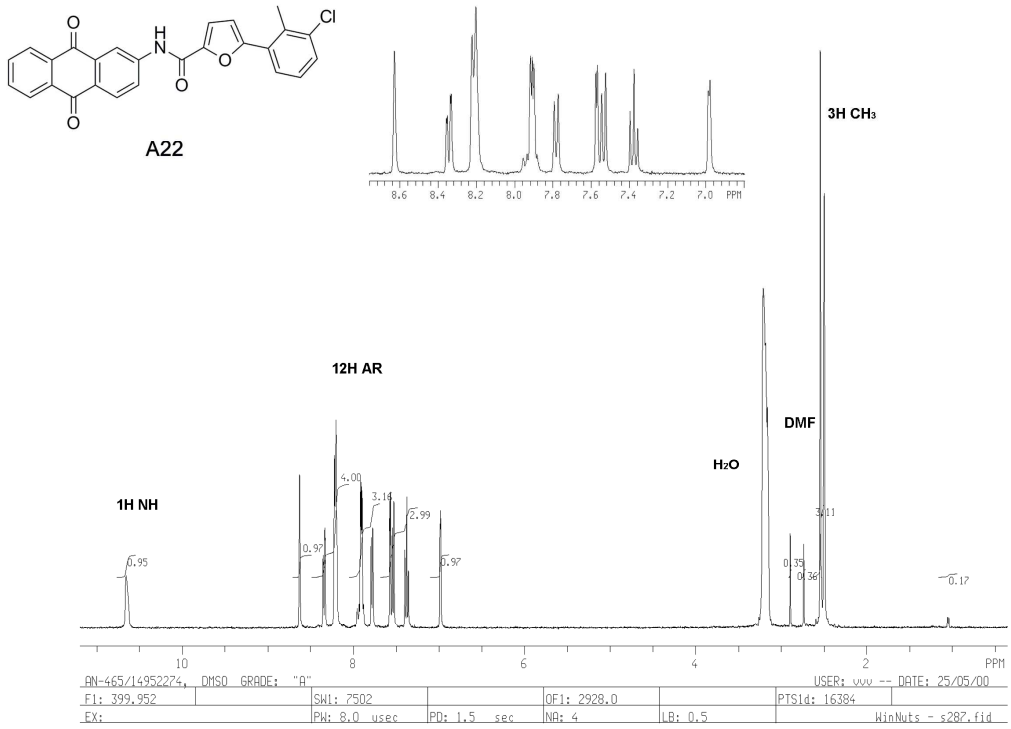

Compound A25

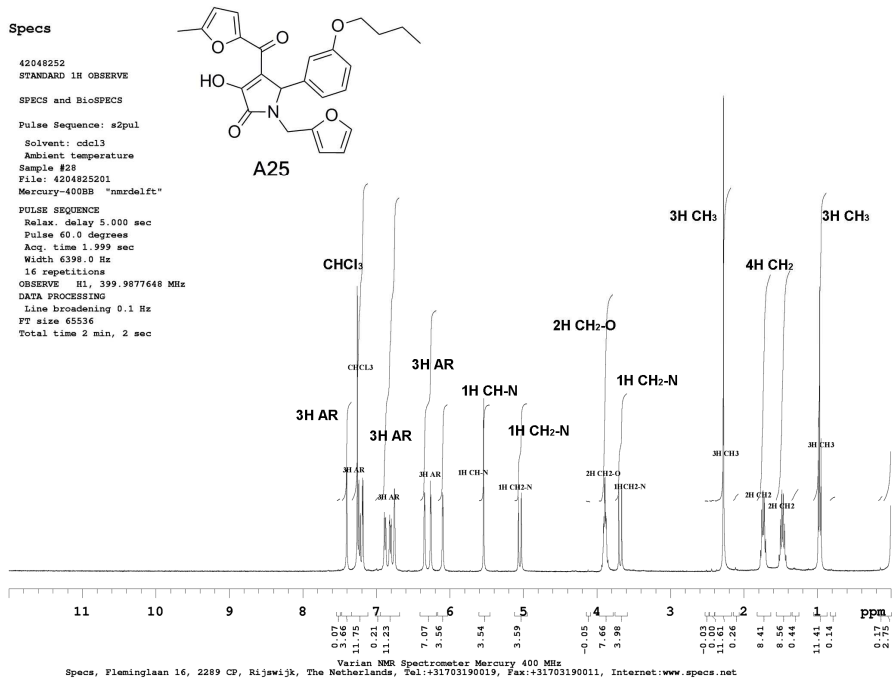

Compound A26

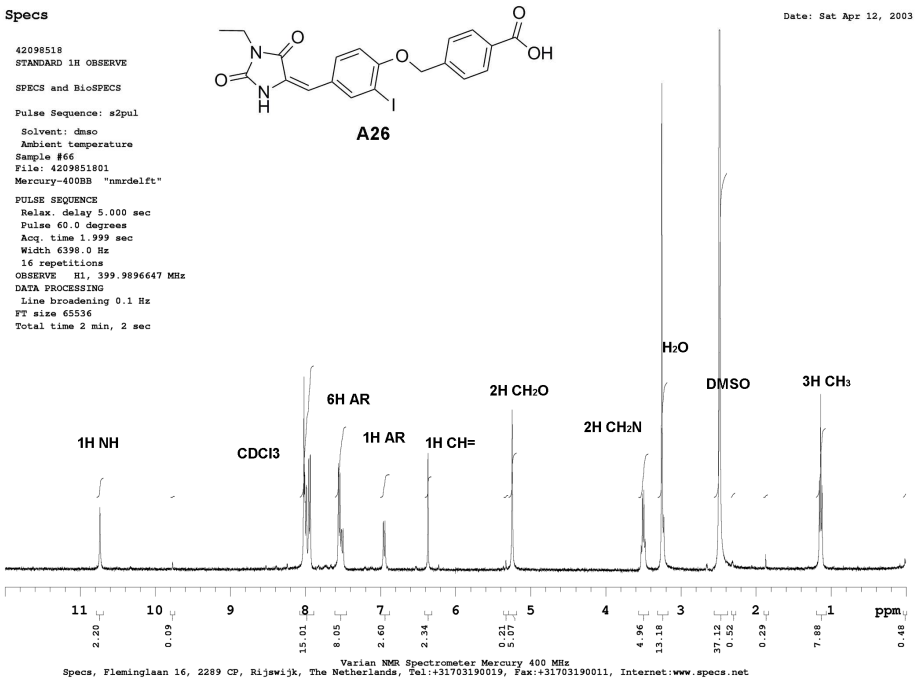

Compound A15-1

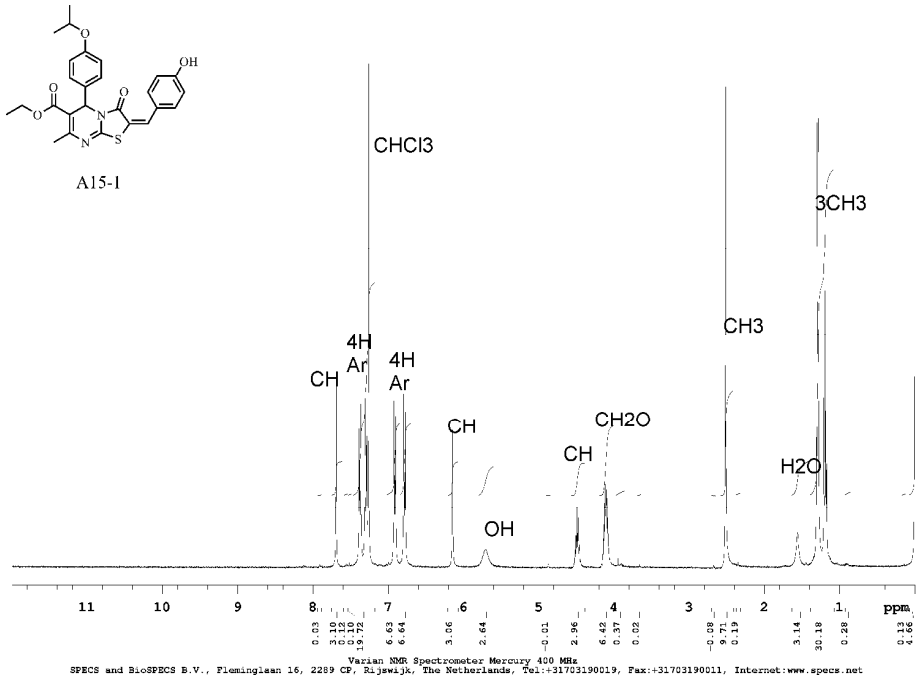

Compound A15-2

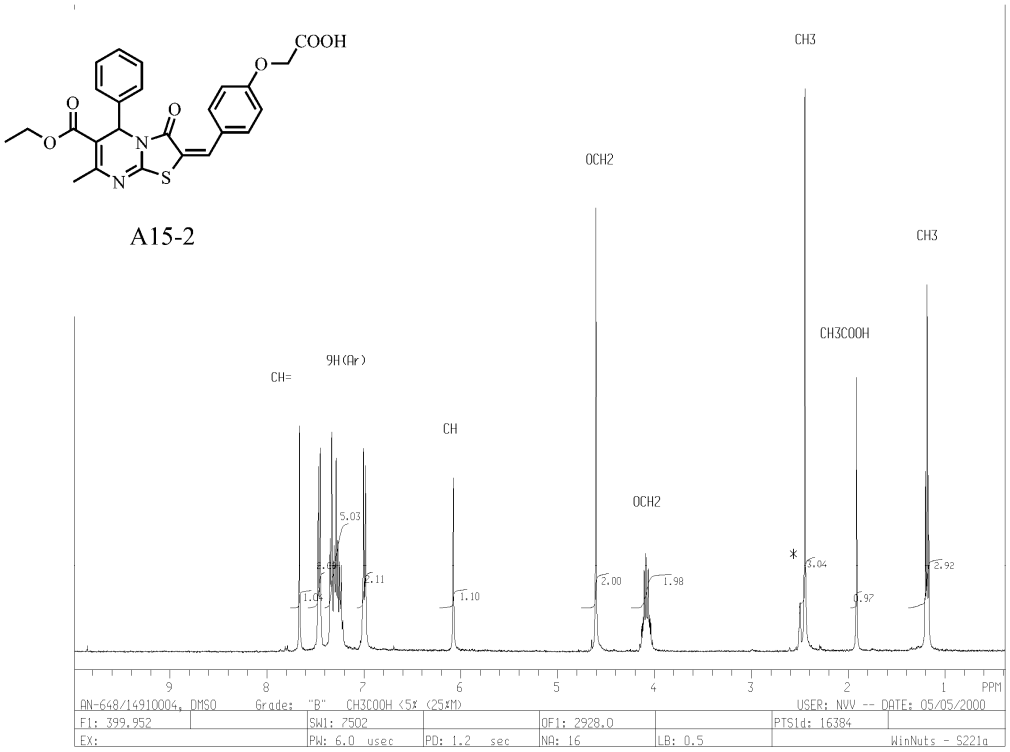

Compound A15-3

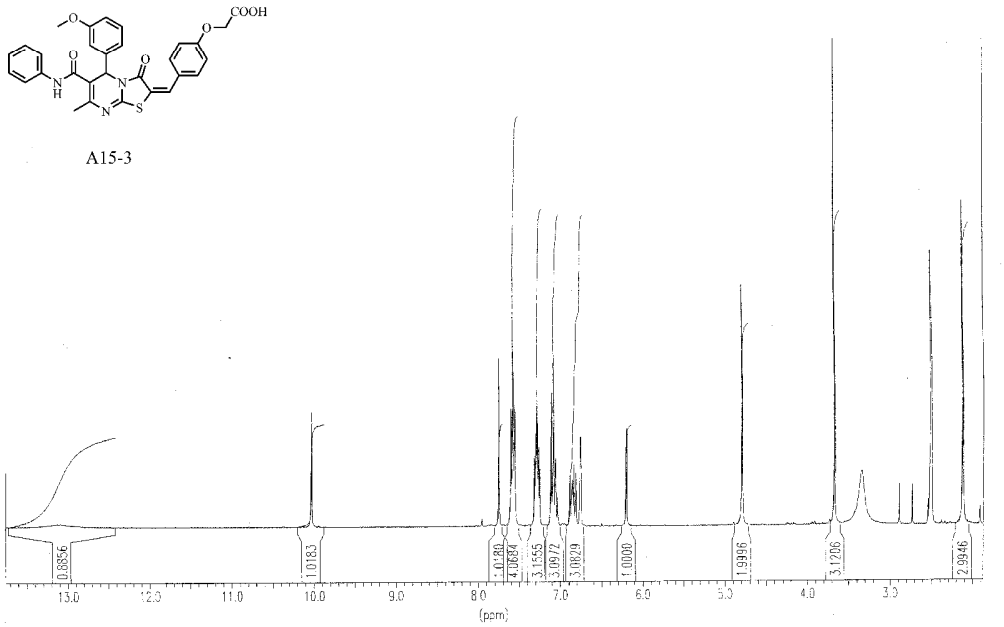

Compound A15-5

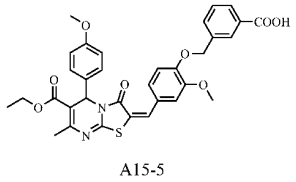

A15-5

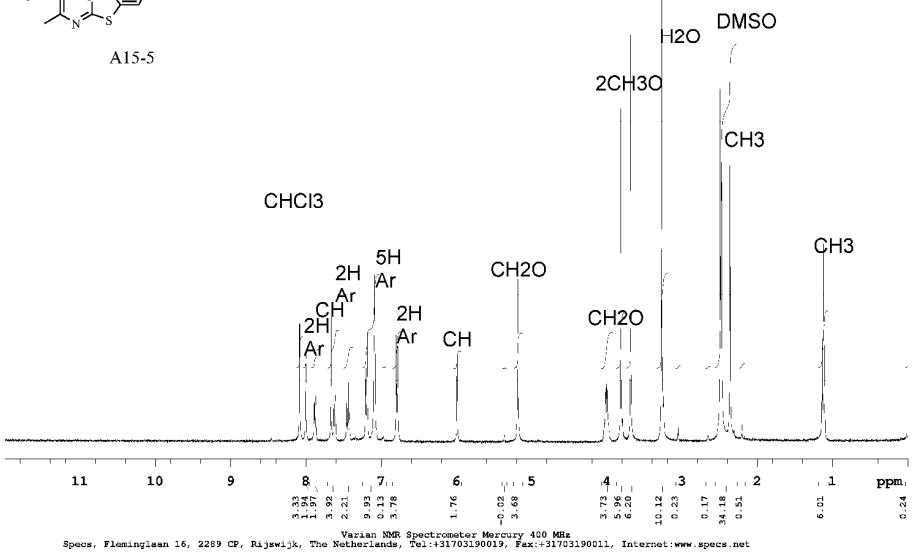

Varian NMR Spectrometer Mercury 400 MHz
Specs, Fleminglaan 16, 2289 CP, Rijswijk, The Netherlands, Tel:+31703190019, Fax:+31703190011, Internet:www.specs.net

Compound A19-1

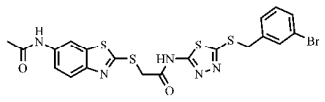

A19-1

Varian NMR Spectrometer Mercury 400 MHz
Specs, Fleminglaan 16, 2289 CP, Rijswijk, The Netherlands, Tel:+31703190019, Fax:+31703190011, Internet:www.specs.net

Compound A19-2

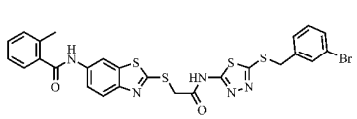

A19-2

Varian NMR Spectrometer Mercury 400 MHz
Specs, Flemminglaan 16, 2289 CP, Rijswijk, The Netherlands, Tel:+31703190019, Fax:+31703190011, Internet:www.specs.net

Compound A19-3

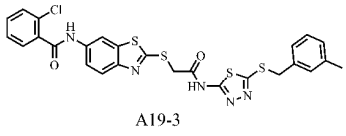

A19-3

Varian NMR Spectrometer Mercury 400 MHz
Specs, Flemminglaan 16, 2289 CP, Rijswijk, The Netherlands, Tel:+31703190019, Fax:+31703190011, Internet:www.specs.net

Compound A19-4

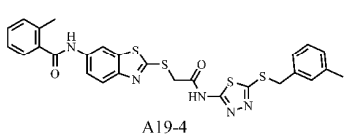

A19-4

Compound A19-6

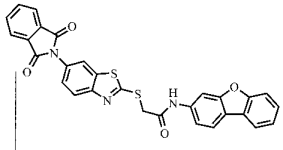

A19-6

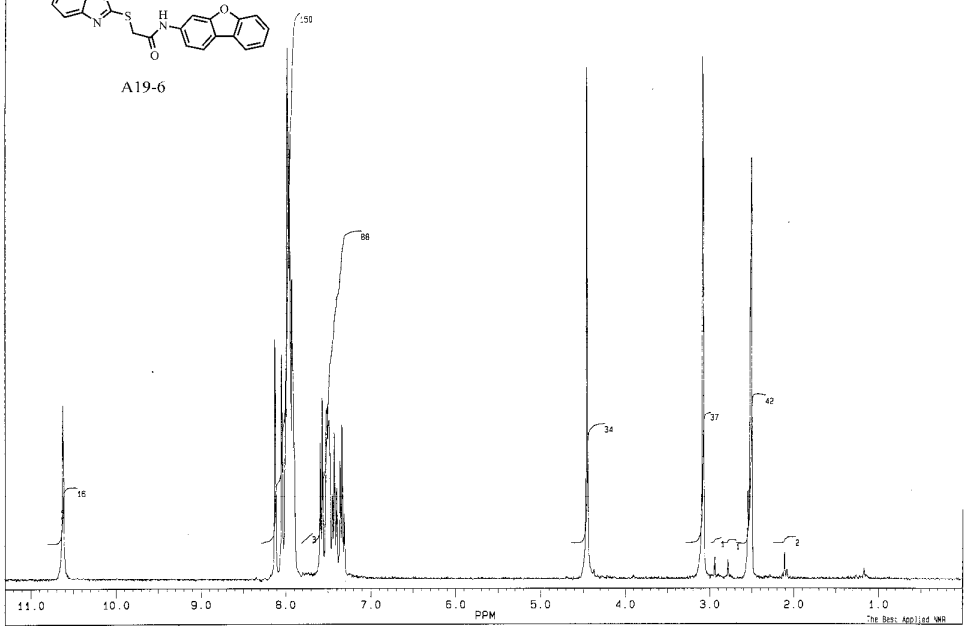

References

1. He, Y.; Liu, S.; Menon, A.; Stanford, S.; Oppong, E.; Gunawan, A. M.; Wu, L.; Wu, D. J.; Barrios, A. M.; Bottini, N.; Cato, A. C.; Zhang, Z. Y. A potent and selective small-molecule inhibitor for the lymphoid-specific tyrosine phosphatase (LYP), a target associated with autoimmune diseases. *J Med Chem* **2013,** 56, 4990-5008.
2. Yu, X.; Sun, J. P.; He, Y.; Guo, X.; Liu, S.; Zhou, B.; Hudmon, A.; Zhang, Z. Y. Structure, inhibitor, and regulatory mechanism of Lyp, a lymphoid-specific tyrosine phosphatase implicated in autoimmune diseases. *Proc Natl Acad Sci U S A* **2007,** 104, 19767-72.
3. Vang, T.; Liu, W. H.; Delacroix, L.; Wu, S.; Vasile, S.; Dahl, R.; Yang, L.; Musumeci, L.; Francis, D.; Landskron, J.; Tasken, K.; Tremblay, M. L.; Lie, B. A.; Page, R.; Mustelin, T.; Rahmouni, S.; Rickert, R. C.; Tautz, L. LYP inhibits T-cell activation when dissociated from CSK. *Nat Chem Biol* **2012,** 8, 437-46.
4. Stanford, S. M.; Krishnamurthy, D.; Falk, M. D.; Messina, R.; Debnath, B.; Li, S.; Liu, T.; Kazemi, R.; Dahl, R.; He, Y.; Yu, X.; Chan, A. C.; Zhang, Z. Y.; Barrios, A. M.; Woods, V. L., Jr.; Neamati, N.; Bottini, N. Discovery of a novel series of inhibitors of lymphoid tyrosine phosphatase with activity in human T cells. *J Med Chem* **2011,** 54, 1640-54.
5. Baldi, P.; Hirschberg, D. S. An intersection inequality sharper than the tanimoto triangle inequality for efficiently searching large databases. *J Chem Inf Model* **2009,** 49, 1866-70.
6. Godden, J. W.; Xue, L.; Bajorath, J. Combinatorial preferences affect molecular similarity/diversity calculations using binary fingerprints and Tanimoto coefficients. *J Chem Inf Comput Sci* **2000,** 40, 163-6.
7. Salim, N.; Holliday, J.; Willett, P. Combination of fingerprint-based similarity coefficients using data fusion. *J Chem Inf Comput Sci* **2003,** 43, 435-42.
8. Cheng, T.; Zhao, Y.; Li, X.; Lin, F.; Xu, Y.; Zhang, X.; Li, Y.; Wang, R.; Lai, L. Computation of octanol-water partition coefficients by guiding an additive model with knowledge. *J Chem Inf Model* **2007,** 47, 2140-8.
9. Tautz, L.; Mustelin, T. Strategies for developing protein tyrosine phosphatase inhibitors. *Methods* **2007,** 42, 250-60.
10. Liu, S.; Zhou, B.; Yang, H.; He, Y.; Jiang, Z. X.; Kumar, S.; Wu, L.; Zhang, Z. Y. Aryl vinyl sulfonates and sulfones as active site-directed and mechanism-based probes for protein tyrosine phosphatases. *J Am Chem Soc* **2008,** 130, 8251-60.